

## Filtering of air through snow as a mechanism for aerosol deposition to the Antarctic ice sheet

Susan L. Harder

Department of Chemistry, University of Washington, Seattle

Stephen G. Warren, Robert J. Charlson, and David S. Covert

Department of Atmospheric Sciences, University of Washington, Seattle

**Abstract.** Aerosol particles serve as cloud condensation nuclei worldwide, and they affect the Earth's radiation budget both directly and indirectly. These particles consist mostly of sulfate compounds. Ice core measurements can be used to infer past variations of atmospheric sulfate concentration, but to do so requires knowledge of the deposition mechanisms. Significant "dry" deposition may occur by filtering when air moves through the snow due to changes in pressure caused by wind blowing over a rough surface (wind pumping). The filtering efficiency of snow was measured at South Pole Station, using an optical particle counter and a condensation nucleus counter. The number size-distribution of ambient aerosol peaks at a dry particle diameter of 0.13  $\mu\text{m}$ , the volume size-distribution at 0.17  $\mu\text{m}$ . Less than 5% of the particles have diameters  $> 0.3 \mu\text{m}$ . Diffusion from interstitial air to snow grains appears to be the primary mechanism of dry deposition for particles  $< 0.6 \mu\text{m}$  in diameter, but another mechanism, probably impaction, becomes significant for larger particles. Aerosol deposition by filtering occurs with an  $e$ -folding time of 1–3 s depending on particle size, corresponding to an  $e$ -folding depth of 0.5–1 cm for an estimated air velocity of 0.4  $\text{cm s}^{-1}$  within the surface snow. Even for long residence times, a small number of particles ( $< 0.1\%$ ) are found in filtered air, suggesting a small degree of new particle formation or reentrainment. However, both the  $e$ -folding depth and the reentrainment rate are small enough that smoothing of the sulfate records in ice cores should be negligible. Three mathematical models for filters agree in describing filtering by snow as dominated by diffusion, but all underpredict the filter efficiency. Capture of aerosol particles is found to be 2–3 times as rapid as that assumed by *Cunningham and Waddington* [1993], supporting their conclusion of nearly total removal of particles from air entering the snow. Blowing snow might also be expected to collect aerosol particles; however, a calculation suggests that deposition to blowing snow on the Antarctic Plateau is insignificant. If wind pumping and diffusion contribute significantly to total deposition, the flux of air into the snow and the residence time of the air within the snow control the deposition rate. Both air flux and residence time are functions of wind speed and surface roughness, so that the aerosol flux to the snow depends on these factors as well as atmospheric concentration, complicating the interpretation of paleoclimate records for aerosol-bound substances.

### Introduction

Sulfate is the main component of cloud condensation nuclei both in remote air and in polluted air [Whitby, 1978; Pruppacher and Klett, 1978]. It is the product of oxidation of biogenic, volcanic, and anthropogenic sulfur emissions and is also a component of sea-salt aerosol. Sulfate is believed to play a major role in the global heat balance and climate by influencing the planetary radiation budget through direct effects (backscattering of sunlight) and indirect effects (cloud albedo and lifetime) [Charlson *et al.*, 1987; Anderson *et al.*, 1992]. Cores from ice sheets contain profiles of sulfate concentration that are thought to reflect the concentration that existed in the atmosphere at the time a given layer of ice was deposited as snow on the surface. These archives show higher

sulfate concentrations during ice ages and lower concentrations during interglacial periods [Legrand *et al.*, 1988; Mayewski *et al.*, 1993] providing further qualitative suggestion of a sulfate-climate connection.

Reconstruction of atmospheric history from ice core profiles is not straightforward. Aerosol particles are introduced into surface snow by "wet" or "dry" deposition mechanisms [Davidson, 1989]. Wet deposition includes incorporation of particles into falling snow and particles serving as condensation nuclei or ice nuclei. Dry deposition describes the incorporation of particles onto or into a snow surface directly by diffusion, impaction, sedimentation, and interception. Interpretation of ice core data, especially over periods of changing snow accumulation rate, depends on the relative contributions of wet and dry deposition. In the hypothetical example of Figure 1 the snow accumulation rate (Figure 1a) suddenly doubles, while the sulfate concentration in air (Figure 1b) remains constant. The variation in time of sulfate archived in the ice (Figure 1c) depends on the relative

Copyright 1996 by the American Geophysical Union.

Paper number 96JD01174.  
0148-0227/96/96JD-01174\$09.00

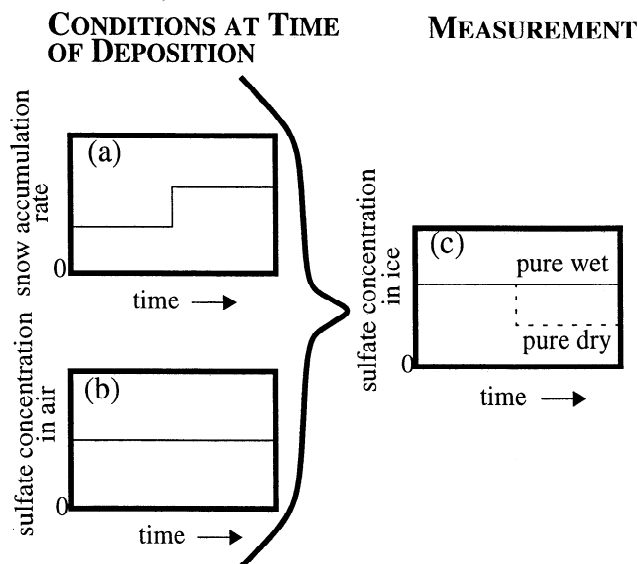


**Figure 1.** Effect of different mechanisms of aerosol deposition on the sulfate record in an ice core, over a time span in which the snow accumulation rate changed while the concentration of sulfate in air remained constant. The resulting concentration of sulfate in the ice is shown for the two extreme cases of pure wet deposition and pure dry deposition, as explained in the text.

contributions of wet and dry deposition. For pure dry deposition, sulfate is deposited at a rate that depends on the concentration in the air. The decrease in sulfate concentration in the ice core can be explained simply as a dilution effect due to greater snow accumulation. For pure wet deposition the sulfate concentration in the ice would be proportional to the concentration in air, independent of the snow accumulation rate, resulting in a constant concentration over the time period. This simple scenario assumes no change in time of the efficiency of wet and dry deposition and assumes that no other factors (e.g., sublimation) act to change the sulfate concentration in the snow after initial deposition. In reality both dry and wet deposition occur simultaneously and the relative contributions of each are likely to vary with time and location. Determining sulfate concentrations in the atmosphere from ice core measurements requires understanding of these mechanisms of deposition and the factors that control them.

The flux of sulfate from the atmosphere to the surface appears to increase with snow accumulation rate as seen in Figure 2, taken from Legrand [1995], indicating a large contribution by wet deposition. The dry deposition flux may be inferred by extrapolation to zero accumulation. Dry deposition becomes relatively more important when snow accumulation is low as for the high plateau locations in the bottom left-hand corner of Figure 2 where dry mechanisms appear to contribute more than half of the total flux. These low-accumulation sites are favored for ice core drilling because of the long period of record available. Legrand [1987] used data from four sites in East and West Antarctica to plot total annual sulfate flux against snow accumulation rate as in Figure 2. He found a linear relationship and, assuming the dry deposition flux to be constant across Antarctica, estimated a dry deposition flux of sulfate from the intercept (at zero snow

accumulation) of  $1.6 \text{ kg SO}_4 = \text{km}^{-2} \text{ yr}^{-1}$ , which at the south pole is about 40% of the total flux. A similar estimate is obtained from Figure 2. Cores from Dome C and Vostok [Legrand and Delmas, 1988, Figure 1; Legrand et al., 1988, Figure 1] differ in their sulfate records, raising questions about the dry deposition mechanisms and the temporal and spatial variation of the factors that control them. These factors include not only the sulfate concentration in air and the snow accumulation rate but possibly also aerodynamic transport, wind conditions, snow microstructure, and surface roughness [Waddington et al., 1996]. Postdepositional changes such as redistribution by drifting, sublimation [Pomeroy et al., 1991], deposition of frost [Bergin et al., 1994, 1995], and reentrainment of particles may also affect the final concentration in ice. Determining an air-snow "transfer function," relating sulfate concentration in ice to that in air, requires an understanding of these processes.

The low rate of snowfall ( $\sim 5 \text{ g cm}^{-2} \text{ yr}^{-1}$  on the East Antarctic Plateau) surely contributes to the relative importance of dry deposition, but in addition, the snow-covered surface of the continent itself may increase the contribution from dry deposition mechanisms. Snow is porous, so that air moves through it, greatly increasing the surface area available for dry deposition over that of a nonporous surface. For snow of density  $0.3 \text{ g cm}^{-3}$ , composed of spherical snow grains of radii  $80 \text{ }\mu\text{m}$ , the surface area  $A_s$  is  $120 \text{ cm}^2 \text{ cm}^{-3}$ . The surface area available for deposition is much greater than that of a planar nonporous surface  $A_p$ ; if aerosols are carried to a depth of  $1 \text{ cm}$ , then  $A_s/A_p = 120$ .

Air moves through the snow due to changes in barometric pressure, surface wind turbulence, and pressure gradients caused by wind blowing over topographic features (wind pumping) [Colbeck, 1989]. Waddington et al. [1996] compared the deposition velocity for aerodynamic transport to the snow surface to that for subsequent ventilation due to wind pumping, determining that the two deposition velocities are of similar magnitude for conditions on the Antarctic Plateau. They concluded that among other processes, ventilation of the snow

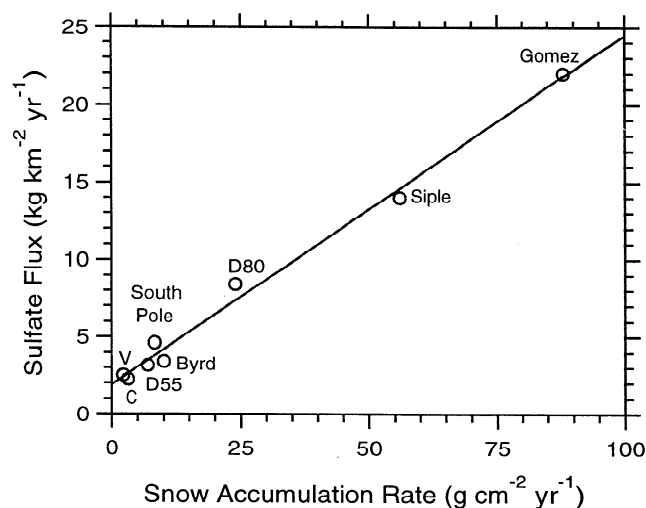


**Figure 2.** Annual flux of non-sea-salt sulfate versus snow accumulation rate, for modern snow at sites in Antarctica. The abbreviations are V for Vostok and C for Dome C (after Legrand [1995]). The value for Gomez is from Mulvaney and Peel [1988].

surface must be understood in order to determine the importance of dry deposition.

The most common topographic features on the polar ice sheets are small longitudinal dunes called sastrugi [Gow, 1965], with typical heights 10-50 cm, widths 1 m, and lengths 1-5 m. Colbeck [1989] and Cunningham and Waddington [1993, hereinafter referred to as CW] have concluded that topographic wind pumping produces the largest flux of air through snow. CW used a three-dimensional model to calculate a volumetric air flux of about  $6 \times 10^4 \text{ m}^3 \text{ m}^{-2} \text{ yr}^{-1}$  at the south pole due to topographic wind pumping, compared to only  $38 \text{ m}^3 \text{ m}^{-2} \text{ yr}^{-1}$  due to barometric pressure changes. To evaluate the importance of wind pumping to total dry deposition, both the air flux and the filtering efficiency of snow for aerosol must be determined. CW used their air flux model together with a model for diffusion of particles to the walls of a tube [Reist, 1993] to estimate a dry flux for non-sea-salt (nss) sulfate of about  $3 \text{ kg SO}_4^{2-} \text{ km}^{-2} \text{ yr}^{-1}$ , which is twice as large as Legrand's estimate, implying that dry deposition may account for most of the total deposition at the south pole.

Experimental studies have been carried out to evaluate the filtering efficiency of snow. Gjessing [1977] found higher ionic concentrations in artificially ventilated snow than in unventilated snow in Norway, and the concentration increased with increasing ventilated air volume. Heintzenberg and Rummukainen (HR) [1993] measured the size distribution for aerosol from 0.1 to 2  $\mu\text{m}$  diameter in ambient air and in air filtered through snow at increasing depths in newly fallen snow in Spitzbergen (Svalbard). Their Figure 6 shows that aerosol concentration decreased exponentially with an  $e$ -folding depth of 2.5 to 4 cm, depending on particle size. HR suggested that filter theory might be used to describe the filtering of aerosol particles by snow. As shown in more detail in the Appendix, filtering is usually described as an exponential decrease in particle concentration with depth,

$$n/n_o = \exp(-\alpha Z), \quad (1)$$

where  $n$  is the filtered particle concentration,  $n_o$  is the ambient particle concentration (at the entrance to the filter),  $Z$  is the length of the filter, and  $\alpha$  is a deposition coefficient in units of inverse length, which depends on particle size. However, HR lacked the additional physical parameters necessary to test a filter theory.

Deposition of aerosol particles may occur to blowing and saltating snow as well as to snow on the ice sheet surface. We observed blowing snow at the south pole about one third of the time during the winter of 1992 and for several days during the summer of 1991-1992. Individual snow grains may remain suspended in the air long enough for significant deposition by diffusion to take place. However, we show below that capture of aerosol particles by blowing snow is insignificant compared to capture by wind pumping.

In this paper we describe snow in the general framework of the theory of filters. We measured the aerosol particle size distribution at the south pole for air drawn through snow filters of various lengths and flow rates. We compare the results to those of the previous experiments of HR and to CW's theoretical model for wind pumping. Three filter-theory models for aerosol deposition are tested using the data, and a temporal deposition coefficient is determined. The filter-theory models, as applied to the typical densities, pore-space sizes, and grain sizes of snow, are examined in detail in the Appendix.

## Field Experiment

### Snow Filter Apparatus

The experiment was conducted at South Pole Station in November 1992 on the border of the designated clean-air sector upwind from the station buildings. Twenty-two snow "filters" of various lengths were constructed by gently pressing clear polyethylene cylinders with sharpened rims into the surface snow. Each filter was removed from the snowpack and its end shaved even with the rim of the cylinder. The individual filters are described in Table 1. The filters were supported horizontally, outdoors to prevent melting. For all experiments the filter temperature was between  $-36^\circ\text{C}$  and  $-44^\circ\text{C}$ , so snow metamorphism during individual experiments was insignificant [LaChapelle, 1992]. The filters were connected with stainless steel tubing to an optical particle counter (OPC) and a condensation particle counter (CPC), housed inside a heated building (Figure 3). Ambient air was measured alternately through a stainless steel intake mounted next to the snow filter. A manually operated valve was used to select the ambient or filtered air.

Particles are measured in 15 size bins from 0.1 to 1.0  $\mu\text{m}$  in effective spherical diameter. A nonspherical particle is represented by the diameter of a sphere of the same projected area. The flow rate for the OPC is maintained with an internal pump and was measured using a rotometer which was calibrated with a bubble flowmeter. The air velocity within the filters is the sum of the volumetric flow for the two particle counters divided by the surface area of the filter corrected for volume fraction of air and was varied using a diaphragm pump following the CPC, producing face velocities at the filter entrance of 0.04-1.42  $\text{cm s}^{-1}$  (Table 1). Total particle concentration and size distribution were measured simultaneously. Each filter measurement was bracketed by measurements of ambient air. Sample time varied from several minutes to several hours depending on length of the filter,

**Table 1.** Snow Filter Experiments

Snow Filter Number	Density, $\text{g cm}^{-3}$	Diameter, cm	Face Velocity, $\text{cm s}^{-1}$	Length, cm	Residence Time of Air, $\text{s}^*$
1	0.30	4.3	0.85	6.4	5.1
2	0.29	4.3	1.17	2.4	1.4
3	0.27	4.3	1.42	2.9	1.4
4	0.31	4.3	1.42	5.9	2.8
5	0.30	4.3	0.99	4.1	2.8
6	0.30	4.3	0.99	6.1	4.1
7	0.33	4.3	0.64	2.6	2.6
8	0.33	4.3	0.64	5.3	5.2
9	0.29	6.0	0.39	12.2	21.4
10	0.35	6.0	0.39	5.7	9.0
11	0.32	7.0	0.24	7.4	20.0
12	0.30	7.0	0.42	7.4	11.9
13	0.30	7.0	0.25	2.0	5.4
14	0.30	7.0	0.25	3.5	9.5
15	0.30	7.0	0.44	3.5	5.3
16	0.30	7.0	0.52	3.5	4.5
17	0.30	7.0	0.04	3.5	58.3
18	0.30	6.0	0.52	4.1	5.3
19	0.39	6.0	0.39	4.1	6.0
20	0.28	6.0	0.39	4.1	7.3
21	0.34	6.0	0.40	3.0	4.7
22	0.45	6.0	0.40	3.0	3.8

\*Residence time = (length x porosity)/face velocity.

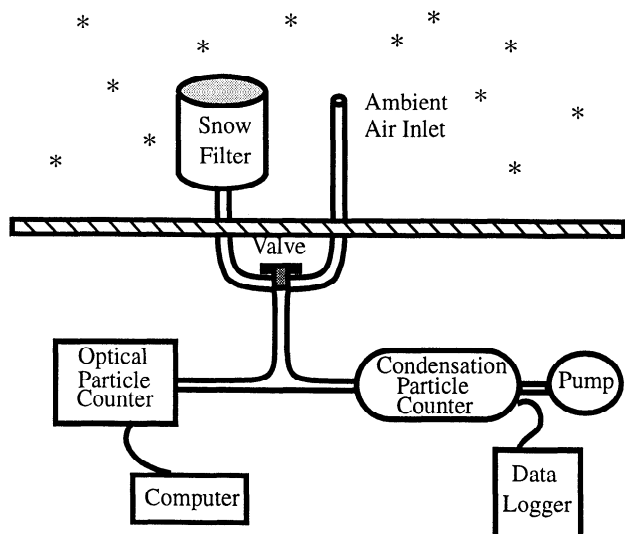


**Figure 3.** Schematic diagram of the snow filtering system at South Pole. The optical particle counter (OPC) was made by Particle Measuring Systems (Boulder, Colorado, model LAS-X-CRT). The flow rate through the OPC was maintained at about  $1.7 \text{ cm}^3 \text{ s}^{-1}$ . The instrument was calibrated in the laboratory with monodispersed  $\text{H}_2\text{SO}_4$  aerosol using an Electrostatic Classifier (Thermal Systems, Incorporated, model 3071, St. Paul, Minnesota) and with latex spheres. (Sulfuric acid was previously determined to be the major component of aerosol at the South Pole [Maenhaut and Zoller, 1979].) Calibration was performed daily in the field using latex spheres and a zero-particle filter. The condensation particle counter (CPC) (Thermal Systems Inc., model 3760, St. Paul, Minnesota) measures the total number of particles with diameters greater than about  $0.014 \mu\text{m}$ . Particle growth is induced by condensation of butanol, and single particles (butanol droplets) are detected by measuring the scattered light with a laser-diode optical detector. The CPC was calibrated using an identical instrument in the laboratory and with a zero-particle filter in the field. The critical orifice was removed from the CPC, and airflow through the instrument and the snow filter was regulated with a battery-powered pump (Gilian Company, Wayne, New Jersey, model HFS113AUP), which was calibrated with a high-resolution rotometer.

flow rate, and the time required to obtain statistically significant counts.

### Snow Structure

Model calculations using filter theory require filter parameters, specifically the dimensions of the filter elements (snow grains), the porosity of the filter, and dimensions of the pore spaces. The porosity  $p$  is the volume-fraction of air:  $p = 1 - (\rho/\rho_{\text{ice}})$ , where  $\rho_{\text{ice}}$  is the density of pure ice ( $0.917 \text{ g cm}^{-3}$ ) and  $\rho$  is the bulk density of the snow. The bulk density  $\rho$  was obtained by simply weighing the snow filters and dividing by the volume of the cylinder.

Samples of snow grains were photographed on a ruler as in Figure 1 of Grenfell *et al.* [1994]. The grains were nearly equidimensional, so that estimates of radii were easily determined. A grain size distribution was produced from the photographs using about 50 measurements (Figure 4a). It is convenient to define an "effective grain radius,"  $R_e$ , to characterize this distribution, which is calculated as follows.

For each of four deposition mechanisms (diffusion, impaction, interception, sedimentation) a weighted mean deposition coefficient  $\bar{\alpha}$  is calculated (see equation (1)), from which  $R_e$  is defined:

$$\bar{\alpha} = \frac{\sum_i \alpha_i f_i}{\sum_i f_i} = \frac{\sum_i K f_i R_i^b}{\sum_i f_i} \equiv KR_e^b, \quad (2)$$

where  $\alpha_i = KR_i^b$  is the deposition coefficient for a given mechanism for the  $i$ th grain-size bin,  $R_i$  is the radius of the snow grain,  $f_i$  is the frequency from the distribution, and  $b$  is an exponent determined from Fuchs' equations, which is different for each deposition mechanism.  $K$  is a collection of coefficients that are independent of  $R$ . In the Fuchs equations for  $\alpha$  we hold the snow density constant as  $R$  varies, by fixing the ratio  $h/R$ , where  $h$  is pore space radius. The values of the exponent  $b$  for diffusion, impaction, interception, and sedimentation are  $-5/3$ ,  $-2$ ,  $-3$ , and  $-1$ , respectively. The effective snow grain radii  $R_e$  are computed from equation (2) to be  $79$ ,  $76$ ,  $70$ , and  $84 \mu\text{m}$ , respectively.

An estimate of pore space radius was obtained using digitized photomicrographs of plane sections of snow from the central plateau of Greenland (Summit site), provided to us by R. E. Davis (personal communication, 1993, 1996). Six micrographs were used for snow with density (about  $0.3 \text{ g cm}^{-3}$ ) and grain radius (about  $100 \mu\text{m}$ ) comparable to those of our snow filters. Multiple, randomly spaced,

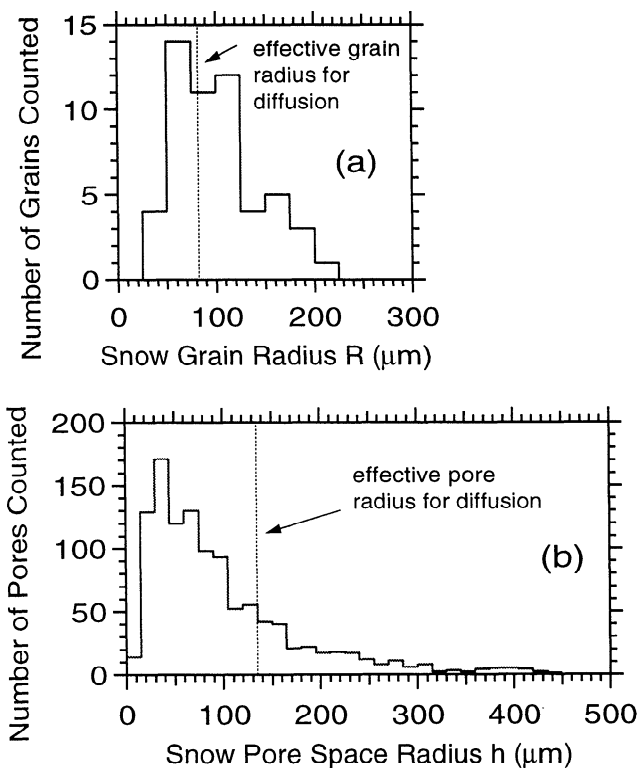


**Figure 4.** (a) Distribution of grain sizes in surface snow at South Pole, measured from photographs. The "effective grain radius" is defined by equation (2). (b) Pore space size distribution in snow from plane section micrographs (supplied by R. E. Davis) of snow from the Summit site on the central plateau of Greenland, similar to snow in experimental filters. The "effective pore radius" is defined in the discussion following equation (3).

horizontal and vertical linear transects were made on each digitized image and the distances between snow grains along these lines were measured, using image processing software developed by *Paddon* [1993]. These intergrain distances were used to construct a distribution of pore space radii (Figure 4b). The image was measured with five transects each in the *X* and *Y* directions giving a total of about 1100 values for the distribution histogram.

An "effective pore space radius" is calculated from the distribution in Figure 4b. If the air in snow were modeled as flow through an assembly of noninterconnecting cylindrical channels, each with a radius  $h_i$  that is constant along its length, then the volumetric airflow would be dominated by the larger tubes, in proportion to  $h_i^4$ , according to Poiseuille's law. This is because the velocity in the tube and the cross-sectional area are both proportional to  $h_i^2$ . An alternative model, of air flowing through a single channel whose width varies along its path in a series of chambers and bottlenecks but again without connections to other channels, would give a velocity proportional to  $h_i^{-2}$  and the volumetric air flux (velocity  $\times$  cross-sectional area) is then proportional to  $h_i^0$ . Neither of these extreme cases applies to snow, because the channels are both varying in width along their length and also interconnected so that bottlenecks can be bypassed. We therefore choose to assume that the air velocity is independent of pore space size, so the pores should be weighted just by the volume of air they contain (and from which aerosol particles will diffuse to the walls of the pore), which is proportional to  $h_i^2$ . This relationship, along with the pore space distribution and a typical snow grain radius of 80  $\mu\text{m}$ , is used to determine a weighted mean deposition coefficient,  $\bar{\alpha}$ , for each of the deposition mechanisms. Thus,

$$\bar{\alpha} = \frac{\sum_i f_i h_i^2 \alpha_i}{\sum_i f_i h_i^2}, \quad (3)$$

where  $f_i$  is the frequency from the distribution and  $\alpha_i$  is the deposition coefficient for pore space  $h_i$  for a particular mechanism. We can define an effective pore space radius ( $h_e$ ), determined by entering  $\bar{\alpha}$  in the appropriate deposition coefficient equation [*Fuchs*, 1964] and solving for the pore space radius. The effective pore space radii for diffusion, impaction, interception, and sedimentation are computed to be 134, 146, 113, and 145  $\mu\text{m}$ , respectively.

## Aerosol Data

Typical number and volume size-distributions of ambient and filtered air, for 0.1- to 1.0- $\mu\text{m}$  particle diameter, are shown in Figure 5. For ambient air the number size-distribution peaks at a diameter of 0.13  $\mu\text{m}$  and the volume size-distribution at 0.17  $\mu\text{m}$ . *Covert and Heintzenberg* [1993] found an accumulation mode peak of 0.22  $\mu\text{m}$  for a number distribution at Ny Alesund (Svalbard), and *HR* found a volume size-distribution peak at 0.35- $\mu\text{m}$  diameter at the same location using similar instruments. The smaller values we find at the south pole are consistent with its location more distant from oceanic and anthropogenic source regions.

Our measurements of total particle concentration at South Pole (diameter  $> 0.014 \mu\text{m}$ ) in ambient air, using the CPC, ranged from  $217 \pm 13 \text{ cm}^{-3}$  (286 at STP) to  $393 \pm 8 \text{ cm}^{-3}$  (523

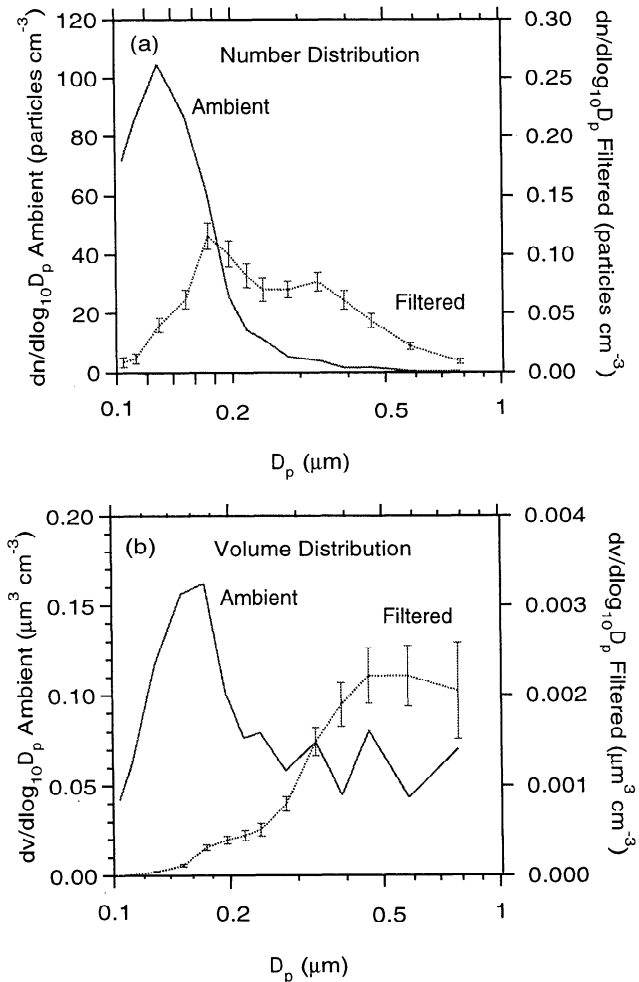


**Figure 5.** (a) Number size-distribution (particles per cubic centimeter at STP) of ambient and filtered air for snow filter 12, whose residence time was 12 s. Maxima are at 0.13 and 0.17  $\mu\text{m}$  diameter. (b) Volume distribution ( $\mu\text{m}^3$  particles /  $\text{cm}^3$  air) of ambient and filtered air for snow filter 12. Maxima are at 0.17 and 0.5  $\mu\text{m}$ .  $D_p$  is particle diameter. The error bars represent the standard error for Poisson counting statistics. Note that the size distributions for filtered air are plotted in expanded scales given in the right-hand axes.

at STP). These values are about 15% higher than those found with an identical instrument located at the Clean Air Facility nearby (*B.A. Bodhaine*, unpublished data, 1992) for the same time period over which our measurements were made. This difference may be due to different amounts of particle loss in the air intake lines of the two systems [*Komhyr*, 1983] or to error in measurement of flow rate. However, our grand mean,  $314 \pm 56$  is significantly higher than values reported by *Hogan* [1979], *Hogan and Barnard* [1978], and *Bodhaine et al.* [1986], all of whom found mean total particle numbers in the range 100-200  $\text{cm}^{-3}$  for the month of November. This difference may be due to volcanic aerosols from the eruptions of Mount Pinatubo and Mount Hudson in 1991, contributing to the aerosol we measured in November 1992.

The previous size distributions measured in Antarctica show clear evidence of two modes. *Shaw* [1988] summarized these results and defined the accumulation mode as the 0.1- to 0.5- $\mu\text{m}$  diameter range, and the Aitken particle mode for

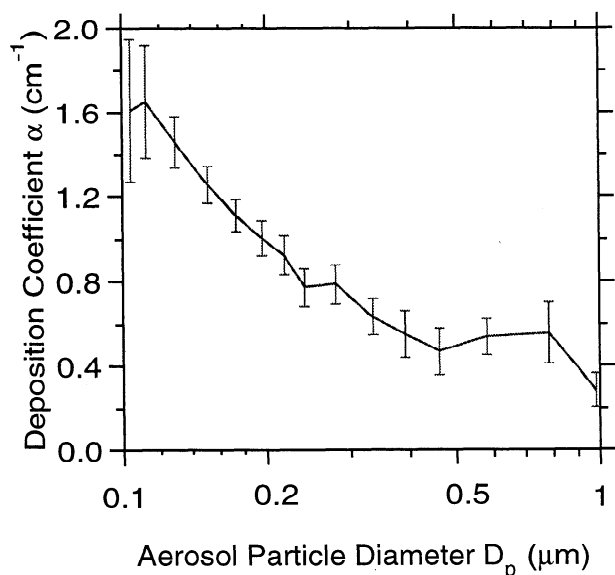


**Figure 6.** The deposition coefficient  $\alpha$  ( $\text{cm}^{-1}$ ) for exponential particle removal for snow filter 22 whose residence time was 4 s. Efficiency of removal decreases with increasing aerosol particle size. Error bars are computed using Poisson counting statistics.

smaller particles. Our distributions measured using the OPC are in the range of the accumulation mode only. However, subtracting the number of particles in the accumulation mode from the total number of particles  $> 0.014 \mu\text{m}$  measured by the CPC gives an estimate of the number of particles in the Aitken mode. We obtain an average number density for the accumulation mode of  $21 \pm 7 \text{ cm}^{-3}$  ( $28 \pm 9 \text{ cm}^{-3}$  at STP) and  $304 \pm 46 \text{ cm}^{-3}$  ( $386 \pm 70$  at STP) for the Aitken mode. Most of the sulfate mass is expected to exist in the accumulation mode [Whitby, 1978].

Figure 5 also displays a typical number and volume distribution for air filtered through snow, on expanded scales given on the right-hand axes. Two features are evident: the magnitude of the particle removal and the shift of the modes. Filters with air residence times greater than 4 s show shifts in the number distribution toward larger particles as seen in Figure 5a. Shifts in the volume distribution shown in Figure 5b are apparent only for residence times greater than 9 s. We interpret these shifts to be due to the greater removal efficiency for the smaller particles, as discussed below.

The deposition coefficient  $\alpha$  (from equation 1), calculated from our experimental data for a typical snow filter, is shown in Figure 6 to decrease with particle diameter, indicating less efficient removal for larger particles. This trend agrees with HR's results and is consistent with the shift to the right seen in the size distributions for filtered air in Figure 5. The actual magnitude of HR's  $\alpha$ , however, was smaller than we obtain, by a factor of about 2. This difference may be due to a higher snow density in our experiment, or to electrical charges on snow grains at our lower temperature, as discussed below.

## Experimental Results Compared to Filter Theory

### Particle Hydration

Comparison of experimental results to filter theory requires knowledge of the aerosol particle size at the filter. This size depends on the amount of hydration which is a function of the

relative humidity ( $RH$ ). The mean  $RH$  in ambient air during the experiments was 97% (computed from dew point temperatures measured nearby by the National Oceanic and Atmospheric Administration) and may be higher within the snow filter, so that some growth may occur as the particle travels through the filter. Growth rate also depends on phase, and particles may be liquid or solid at the temperatures within the filter ( $-40^\circ\text{C}$ ), so the exact particle size at the time of deposition is difficult to determine. The particles measured in the OPC are "dry" due to evaporation of water as the particle warms by about 60 K as it travels from the filter ( $T \approx -40^\circ\text{C}$ ,  $RH \approx 100\%$ ) to the instrument ( $T \approx +20^\circ\text{C}$ ,  $RH \approx 5\%$ ). We provide indirect evidence below that the particle diameter during filtration is about 4 times the dry diameter.

### Filter Theory and Experimental Results

Filter theory predicts a reduction of aerosol particle number-concentration exponentially with distance along the filter, so that the survival fraction of particles is expressed as

$$n/n_0 = \exp(-\alpha Z) = \exp(-Z/\sigma), \quad (4)$$

where  $Z$  is the thickness of the filter and  $\sigma = 1/\alpha$  is the average survival distance for an aerosol particle moving through a filter. As shown in the Appendix, filter theory predicts that diffusion will be the dominant mechanism of deposition for particles in the accumulation mode in filters with grain size and pore space sizes characteristic of snow. Deposition by diffusion, however, reduces particle number exponentially with time even in stagnant air. Where diffusion dominates, it is therefore appropriate to express the survival fraction instead as

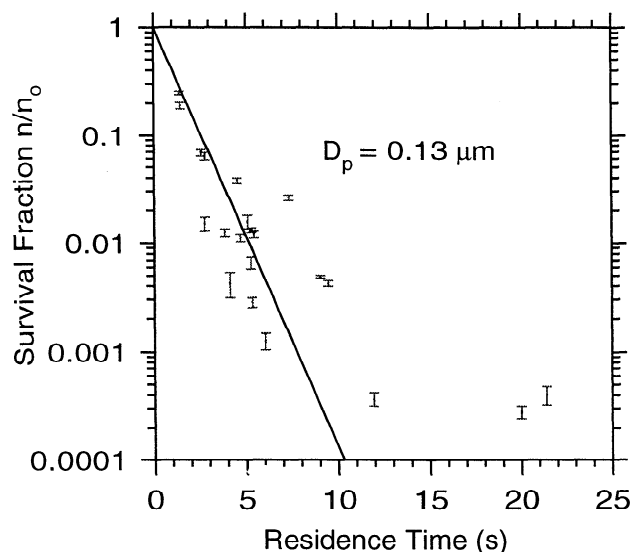


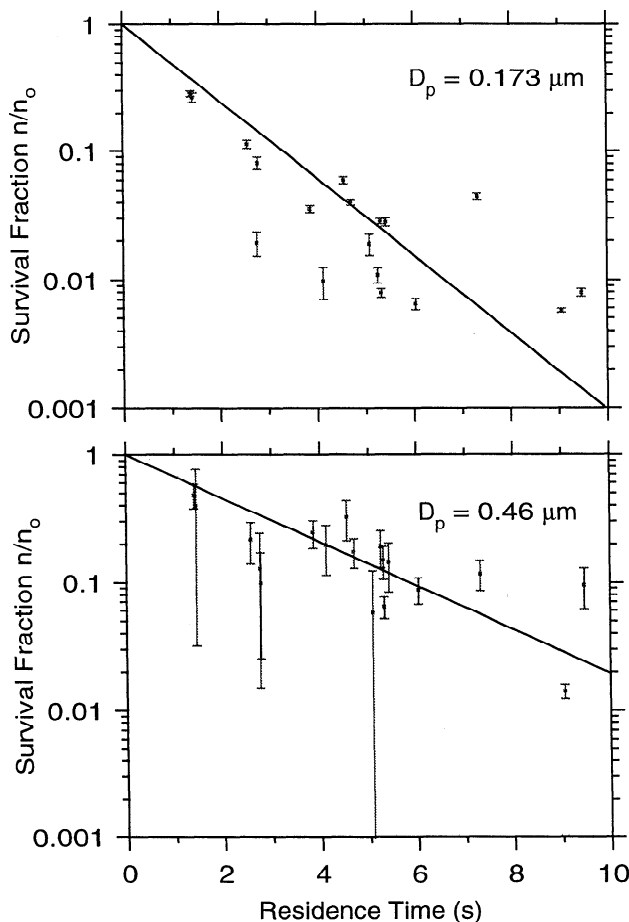
**Figure 7.** The survival fraction  $n/n_0$  is plotted versus residence time for 21 snow filters for aerosol particle diameter  $D_p = 0.13 \mu\text{m}$  (the peak of the number distribution). The fraction  $n/n_0$  decreases exponentially with residence time for  $t < 10$  s. However,  $n/n_0$  did not decrease further in the filters with residence times near 20 s. The survival fraction for filter 17 (residence time  $\sim 60$  s) was a factor of 10 larger than for filters with residence times of 12 and 20 s, suggesting a fault in the experiment such as a crack developing in the filter which would allow greater particle survival. That point is not included here. The straight line is a fit to points with residence times less than 10 s.

$$n/n_0 = \exp(-t/\tau), \quad (5)$$

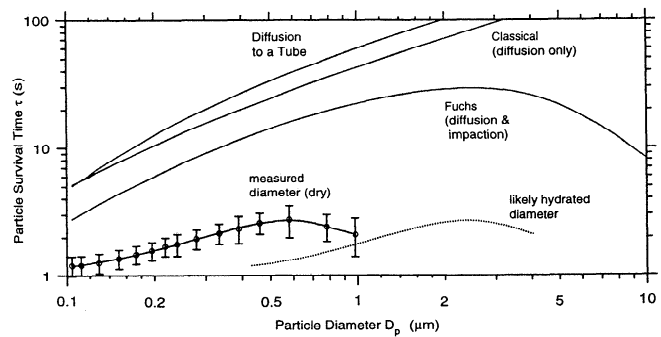
where  $t$  is the residence time for a parcel of air in the filter (the time required for air to traverse the filter) and the "survival time"  $\tau$  is the average lifetime of an aerosol particle in the interstitial air within the filter before diffusion to and capture by the filter material.

Figure 7 shows  $n/n_0$  versus residence time for 21 filters for the peak of the number distribution,  $D_p = 0.13 \mu\text{m}$ . The fraction  $n/n_0$  decreases with increasing residence time for  $t < 10$  s and then makes a transition to a constant regime for  $t > 10$  s. Although near-total removal (about 99.95%) is observed in this regime ( $t \gg \tau$ ), a very small number of particles continue to emerge downstream of the filter for residence times of about 20 s. This result is consistent with Gjessing's [1977] finding of incomplete filtration for a 1-m layer of snow and suggests the possibility of formation of new particles, or reentrainment of particles at a small rate. However, this rate is small enough that it is negligible for most purposes.

Since diffusion is expected to be the dominant mechanism of deposition for submicrometer particles, a linear fit should be obtained when  $\log(n/n_0)$  is plotted versus  $t$  (equation 5). Some examples are shown in Figure 8 for experiments with residence times  $< 10$  s;  $\tau$  is obtained from the slope of the line.



**Figure 8.** The survival fraction  $n/n_0$  as a function of residence time  $t$  (for  $t < 10$  s). Each snow filter is represented by one point. Least squares fits are shown for two aerosol particle sizes, where the slope of the line is  $-\tau^{-1}$  (equation (5)). The survival time  $\tau$  is greater for larger particles.



**Figure 9.** Particle survival time  $\tau$  (equation (5)) as a function of particle diameter  $D_p$  for experimental data and for model predictions of classical theory, diffusion within a tube, and Fuchs' theory. The solid lines represent experimental and theoretical results. The dotted line shows the experimental curve for the diameter expanded from the measured "dry" diameter to a hydrated diameter larger by a factor of 4. Error bars show the uncertainty in  $\tau$  due to uncertainty in the least squares slopes such as shown in Figures 7 and 8. Experimental  $\tau$  increases with  $D_p$  up to  $0.58 \mu\text{m}$  indicating that diffusion is the dominant deposition mechanism. For  $D_p > 0.58 \mu\text{m}$  another mechanism apparently becomes significant. The three theories predict much longer survival times than indicated by the experimental data.

These survival times are then plotted as a function of particle size in Figure 9. The lower solid curve is the experimentally determined survival time as a function of the measured dry diameter. This curve is shifted to the right (dotted curve) to show  $\tau$  for hydrated particles larger by a factor of 4. The positive slope exhibited on the left portion of the curve is expected for deposition dominated by diffusion since only for diffusion does filter efficiency decrease with increasing particle size (Appendix). The negative slope at the right end of the curve suggests that another mechanism, probably impaction, becomes significant for the larger particles. The peaks of both the number distribution and the volume distribution (dry diameters of  $0.13$  and  $0.17 \mu\text{m}$ , respectively) fall within the diffusion-dominated portion of the curve, indicating that diffusion is the major deposition mechanism for accumulation-mode particles in air flowing through snow.

We also have theoretically estimated the particle survival time  $\tau$ , for the experimental conditions corresponding to each snow filter, for three models: Fuchs' theory for low-porosity filters [Fuchs, 1964], classical theory for high-porosity filters represented by Langmuir's model [Fuchs, 1964], and a model for deposition to the walls of a tube used by CW [Reist, 1993, p. 154]. Diffusion, impaction, interception, and sedimentation are combined here for Fuchs' model by simply adding the deposition coefficients, resulting in a lower limit for  $\tau$ . The model for deposition to a tube and Langmuir's classical model are for diffusion only. The theoretical curves trace the midpoints of the range for each particle size computed for conditions present in the experimental filters.

The theoretical curves (Figure 9) agree with experimental results in predicting diffusion as the principal mechanism of deposition for submicrometer particles. However, their predicted survival times are longer than those found experimentally. Increasing the particle diameter by a factor of 4 to simulate hygroscopic growth moves the experimental curve to the right into closer agreement with Fuchs' theory

with respect to the position of the peak (although worse agreement with respect to the magnitude of  $\tau$ ), suggesting that the hydrated particle diameter may be 4 times as large as the measured dry diameter. This hydration factor is only a rough estimate because of uncertainty in the values used for the model parameters and because the model result has a broad maximum so that the location of its peak is not well defined. For a hydration factor of 4, our experimental  $\tau$  is about a factor of 10 smaller than given by Fuchs' theory. One possible explanation for the discrepancy is that snow grains retain static electrical charges at temperatures characteristic of our experiments ( $-36^\circ$  to  $-44^\circ\text{C}$ ), which would allow directed migration of aerosol particles faster than by passive diffusion. This effect may contribute to the greater filtering efficiency of south polar snow in comparison to the snow at Spitzbergen studied by HR, which was probably warmer.

Another possible explanation relates to the tortuosity of the pathway the air takes through the filter, but we will argue that tortuosity cannot explain the discrepancy. The calculations for Figure 9 assume a straight-line path, so that the distance the air travels within the filter is just the length of the filter. In reality the flow lines curve around snow grains so that the path length and therefore the residence time become longer. If we define a tortuosity factor  $\xi$  as the ratio of the length of the air path through the filter to the length of a straight-line path, the residence time  $t$  that we computed should be increased by this factor. The survival time  $\tau$  that we obtain (equation 5) would be larger by the same factor. All calculations here have assumed  $\xi = 1$ . To obtain agreement with Fuchs' theory (using the hydrated diameters) would require  $\xi \approx 10$ . However, inspection of Davis' photomicrographs of Greenland snow suggest  $\xi < 2$ , so that tortuosity is not likely to account for the difference between experimental and theoretical survival times.

## Dry Deposition of Aerosols to the Antarctic Plateau

### Wind Pumping

Cunningham and Waddington (CW) [1993] developed a model for deposition of aerosol particles by wind pumping due to laminar airflow over snow dunes and sastrugi. Wind blowing over surface topography causes pressure perturbations which force air into surface depressions and out of surface ridges. CW modeled topographic features as three-dimensional sinusoids and, using Darcy's law with Colbeck's [1989] equation for pressure perturbation, determined a volume flux for air into snow. They combined this air flux model with the model for diffusive deposition to the walls of a tube [Reist, 1993] to estimate the dry deposition flux of sulfate aerosol to the snow surface. This model is shown in Figure 9 to underpredict the filtering efficiency of snow. Accordingly, CW's model also underpredicts deposition when compared to our experimental results. Filter efficiency, defined as the fraction of particles removed from the airstream ( $1 - n/n_0$ ), or  $1 - e^{-t/\tau}$  (equation 5), is plotted as a function of residence time in Figure 10. The bottom solid line is copied from CW's Figure 8 and represents CW's results for an aerosol particle  $0.1 \mu\text{m}$  in diameter flowing through a tube  $180 \mu\text{m}$  in radius. Our experimental results are calculated using  $\tau$ , from Figure 9, for each particle size. The upper boundary of the shaded area corresponds to the smallest size measured,  $D_p = 0.1 \mu\text{m}$ , the

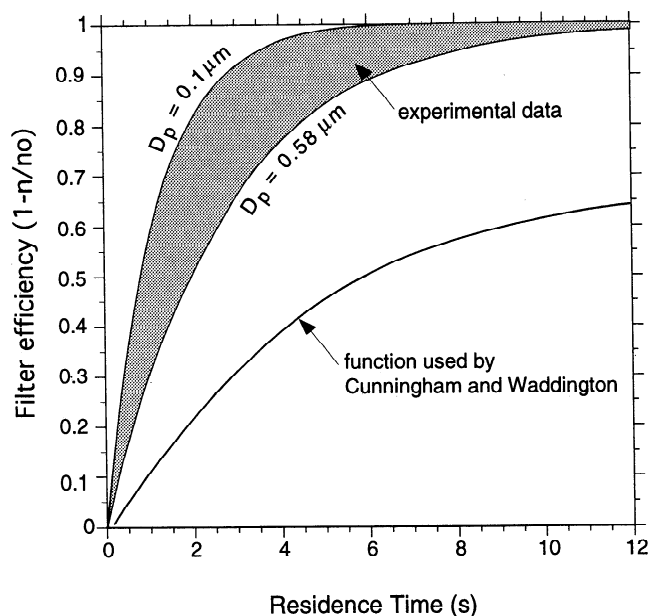


**Figure 10.** The dependence of snow filter efficiency on residence time. Filter efficiency is defined as the fraction of particles retained by the filter, i.e.,  $1 - n/n_0$  or  $1 - e^{-t/\tau}$ . The shaded region is experimental data. The upper boundary of the area is determined by aerosol particles of  $0.1 \mu\text{m}$  diameter (the smallest size measured) and the lower boundary by the particles with maximum  $\tau$ ,  $0.58 \mu\text{m}$  diameter. The solid line is the function used by Cunningham and Waddington [1993] in their model for south polar snow.

lower boundary to the particle size with maximum  $\tau$ ,  $D_p = 0.58 \mu\text{m}$ . CW used the hydraulic radius  $180 \mu\text{m}$  [Carman, 1956], estimated from porosity and permeability measurements on south polar snow as representative of the pore space. Our estimate for effective pore space radius is  $134 \mu\text{m}$  as discussed above.

CW's model thus underestimates filtering efficiency for all residence times. However, for topography that they consider to be typical of the south pole (sinusoidal features representative of sastrugi, with amplitude  $0.1 \text{ m}$ , down-wind length  $1.4 \text{ m}$ , and cross-wind width  $0.7 \text{ m}$ ), CW's air flux model predicts sufficiently long residence times that nearly all the particles are removed in spite of the low efficiency. An increase in filter efficiency will increase the final estimate for sulfate flux only if residence times are significantly shorter than CW computed; for example, if the topographic features at the south pole are smaller than they assumed. Therefore, contingent on the accuracy of CW's air flux model, our measurements confirm their conclusion that air entering snow due to wind pumping will be essentially cleansed of particles. Their estimate for sulfate aerosol flux by this process was about  $3 \text{ kg SO}_4^- \text{ km}^{-2} \text{ yr}^{-1}$  (Figure 9 of CW), assuming a mean annual air concentration of  $100 \text{ ng SO}_4^- \text{ m}^{-3}$  (STP). This flux is about  $2/3$  of the total deposition of sulfate at the south pole (Figure 2), implying that most of the aerosol deposition could be due to wind pumping. The volumetric air flux, and thus the aerosol deposition rate, is proportional to the square of the wind speed  $u$  (CW, equation 35). A 40% increase in  $u$  could thus cause a doubling of the sulfate flux to the snow, assuming the concentration of sulfate in the air entering the snow remains constant. CW therefore concluded that variations of

**Table 2.** Permeability Measurements of South Polar Snow

Sample Number	Description	Permeability, $10^{-10} \text{ m}^2$
1	hard surface, wind packed, $r = 0.4 \text{ g cm}^{-3}$	8.6
2	hard surface, wind packed, duplicate of 1	7.9
3	new drift, 2.5 cm crust	5.9
4	new drift, 2.5 cm crust over 2.5 cm soft snow	6.3
5	small sastruga, 6-11 cm depth	12.1
6	small sastruga, 6-11 cm depth	13.3
7	small sastruga, top 6 cm	8.5
8	long sastruga, top 2 cm, soft, center	8.8
9	long sastruga, top 2 cm, soft, windward end	10.2
10	long sastruga, top 2 cm, soft, lee end	12.4
11	long sastruga, hard snow below 2 cm	8.5
12	long sastruga, hard snow below 2 cm	8.4
13	long sastruga, center, 6-11 cm	8.4
14	short sastruga, depth hoar at 3 cm	17.7
15	short sastruga, 8 cm depth	14.7
mean		10.1

wind speed and sastrugi height during the ice ages could account for the observations of sulfate variation in ice cores.

However, CW used an intrinsic permeability for snow of  $40 \times 10^{-10} \text{ m}^2$  in their model calculations. We measured the permeability of surface snow at the south pole (Table 2) and obtained values that are a factor of 4 smaller than those used by CW. The snow surface of an ice sheet is often a wind crust in which pore spaces are clogged by blowing snow, so that the permeability can be as much as a factor of 10 smaller at the surface than at 1-m depth [Albert *et al.*, 1996]. The value of permeability used by CW is probably appropriate for the deeper firn, but wind pumping is limited by the permeability of the surface wind crust. If we reduce the permeability by a factor of 4 in CW's model, the air flux and sulfate deposition would also correspondingly diminish by a factor of 4, thereby decreasing the significance of ventilation as a mechanism for dry deposition.

The permeability may undergo changes during ice age cycles. The thin surface crust of low permeability forms during the summer when the air temperature is high enough for surface snow grains to bond tightly by sintering. Lower air temperatures during glacial periods might inhibit the formation of this crust, allowing the surface snow to remain highly permeable during summer, the season of highest atmospheric sulfate concentration. This change of permeability alone could cause greater deposition of sulfate into ice age snow.

Wind pumping affects not only the amount of sulfate deposited but also the vertical resolution (and therefore the time resolution) of snow (and ice core) profiles. The survival time  $\tau$  can be used, together with CW's estimate of natural air velocity within the snow of about  $0.4 \text{ cm s}^{-1}$ , to calculate an  $e$ -folding depth. For particles from 0.1 to  $1 \mu\text{m}$  diameter the  $e$ -folding depth is 0.5-1 cm. Annual snow accumulation at the south pole and Vostok is about 8 and  $2.5 \text{ g cm}^{-2} \text{ yr}^{-1}$ , respectively, which corresponds to  $2.2$  and  $0.7 \text{ cm month}^{-1}$  for snow with an average density of  $0.3 \text{ g cm}^{-3}$  [Schwerdtfeger, 1984; Young, 1982]. Therefore the limit to resolution, resulting from wind pumping processes alone, for ice core time series should be on the order of a few months. However, drifting of snow may redistribute surface layers to a greater

depth and may be a more important factor in limiting resolution.

Since sastrugi are sometimes higher than the annual snow accumulation, if wind pumping produces significant deposition to selected areas of the snow surface, then a loss of the annual cycle might be expected for sulfate. The annual signal is, however, well preserved in snow pits and cores. This puzzle was addressed by Gow [1965] in his studies of snow accumulation and stratigraphy at the South Pole. He found that most of the precipitation fell in the autumn and winter and that sastrugi development is greatest at the end of winter. During the summer the surface snow is redistributed and leveled by processes of sublimation, surface hoarfrost formation, and drifting snow. Gow stated that the "generally uniform stratigraphy in pits of the South Pole can be attributed in large part to a gross leveling of this surface relief during the summer by a process of sublimation-deflation. The ultimate result is to redistribute the snow more uniformly over the surface. It is on this substantially level surface, evident at the end of summer, that the new year's accumulation will be deposited." This level surface is topped by a hard crust that forms in late summer and resists erosion by wind. Thus the sastrugi that form in winter consist of snow from only that winter and are destroyed by the leveling process that creates the annual layer. This same process would preserve the annual signal for sulfate.

### Diffusion of Particles to Blowing Snow

When the wind speed exceeds about  $7 \text{ m s}^{-1}$ , enough snow grains are lifted from the surface to above eye level that the sky is visually obscured. At South Pole this condition is rare in summer but common in winter, so that over the course of a year it occurs about one quarter of the time. If diffusion is the primary mechanism for deposition of submicrometer aerosol particles, then deposition to blowing snow may be significant, because blowing snow represents additional area to which aerosol can diffuse. An order-of-magnitude estimate of this deposition can be made by calculating the rate of diffusion of aerosol particles to the surface of a sphere [Fuchs, 1964, eq. 38.36].

The deposition rate  $\Phi_{ij}$  (particles per second) for aerosol of size class  $i$  to blowing snow grains of size class  $j$  is

$$\Phi_{ij} = 4\pi D_i R_j n_i \quad (6)$$

where  $D_i$  is the diffusion coefficient ( $\text{m}^2 \text{ s}^{-1}$ ) for aerosol particles of size class  $i$ ,  $R_j$  is the radius of the blowing snow grain, and  $n_i$  is the number density of aerosol particles (of class  $i$ ) in ambient air. The corresponding mass flux  $F_{ij}$  ( $\text{g s}^{-1}$ ) is

$$F_{ij} = \Phi_{ij} m_i = 4\pi D_i R_j n_i m_i \quad (7)$$

where  $m_i = (4/3)\pi r_i^3 \rho_p$  is the mass of an aerosol particle of radius  $r_i$  and density  $\rho_p$ . (Here we assume the aerosol consists solely of sulfuric acid with a density of  $1.84 \text{ g cm}^{-3}$ .) The mass flux of all aerosol collected by a snow grain of size  $j$  is

$$F_j = \sum_i F_{ij} = 4\pi R_j \sum_i D_i n_i m_i \quad (8)$$

The mass fraction of sulfuric acid in a single blowing snow grain, due to diffusion, assuming the aerosol is pure  $\text{H}_2\text{SO}_4$ , is

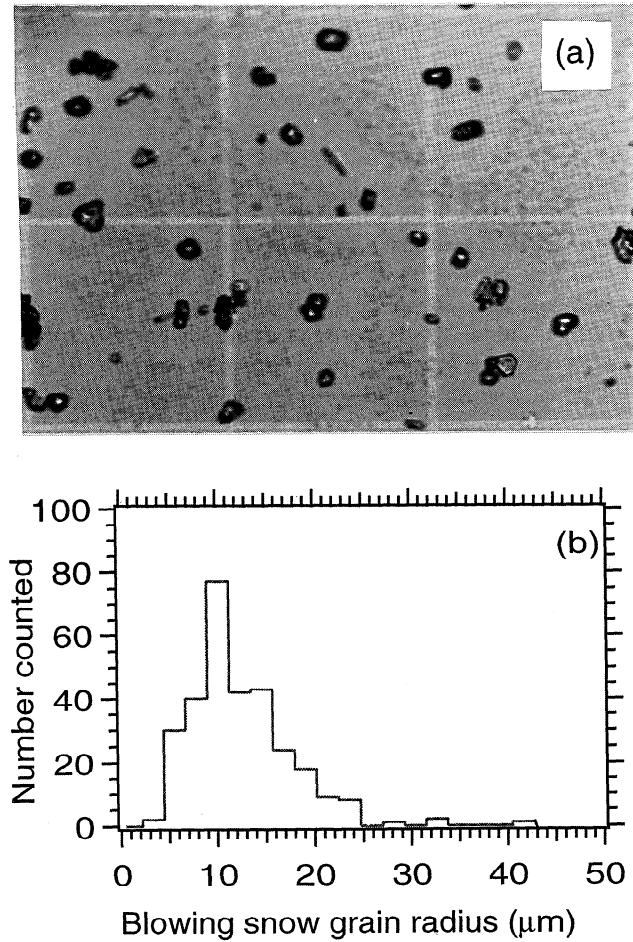


**Figure 11.** (a) A portion of a photomicrograph of blowing snow taken at the South Pole in July 1992. The grid spacing is 250 μm. (b) Size distribution obtained from the photomicrograph. The effective radius (equation (12)) is  $R_e=15$  μm.

$$C_j = F_j t / M_j, \quad (9)$$

where  $t$  is the time the snow grain remains suspended in air and  $M_j = (4/3)\pi R_j^3 \rho_{\text{ice}}$  is the mass of the snow grain, where  $\rho_{\text{ice}}$  is the density of ice. Thus

$$C_j = (4\pi t / R_j^2) (\rho_p / \rho_{\text{ice}}) \sum_i D_i n_i r_i^3. \quad (10)$$

The average mass fraction  $\bar{C}$  is then

$$\bar{C} = \sum_j C_j n_j M_j / \sum_j n_j M_j = (4\pi t / R_e^2) (\rho_p / \rho_{\text{ice}}) \sum_i D_i n_i r_i^3, \quad (11)$$

where we have defined an "effective radius"  $R_e$  of the blowing snow as

$$R_e^2 = \sum_j n_j R_j^3 / \sum_j n_j R_j, \quad (12)$$

where  $n_j$  is the number density of blowing snow grains of size class  $j$ .

The size distribution  $n_j$  of blowing snow grains (approximated as spheres) is obtained by measurements on a photograph of blowing snow collected on a microscope slide during a blizzard at South Pole in July 1992 (Figure 11), giving  $R_e = 15$  μm for a winter distribution. The blowing snow particles are larger in summer, so for summer we estimate  $R_e = 30$  μm.

For the aerosol size distribution  $n_i$  in summer we use the values for ambient air measured in November 1992, but to represent a winter value, we decrease  $n_i$  by a factor of 10 for all sizes [Bodhaine *et al.*, 1986]. The diffusion coefficient  $D_i$  is calculated from Fuchs [1964, eq. 35.2] using not  $r_i$  but rather the estimated hydrated particle size  $4 r_i$  as discussed above. The time  $t$  that an average snow grain remains suspended is

$$t = f B / A = \delta f H / A, \quad (13)$$

where  $A$  is the average snow accumulation ( $\text{g m}^{-2} \text{month}^{-1}$ ),  $f$  is the fraction of time in that month that snow is blowing, and  $B$  is the column burden ( $\text{g m}^{-2}$ ) of blowing snow, equal to the

**Table 3.** Deposition of Aerosol Particles by Diffusion to Blowing Snow at the South Pole

Input to Calculation	Winter (March-October)	Summer (November-February)
Effective radius $R_e$ of blowing snow grains, equation (12)	15 μm	30 μm
Density of blowing snow $\delta$	1 g m <sup>-3</sup>	1 g m <sup>-3</sup>
Scale height $H$ of blowing snow	200 m	20 m
$D_p(\text{wet}) / D_p(\text{dry})$	4	4
Snow accumulation <sup>a</sup>	0.8 g cm <sup>-2</sup> month <sup>-1</sup>	0.4 g cm <sup>-2</sup> month <sup>-1</sup>
Fraction of time snow is suspended in air <sup>b</sup>	0.25	0.075
Time snow spends in air	5 hours	0.3 hours
Aerosol number concentration	10% of summer values <sup>c</sup>	Mean measured with OPC, November 1992
<b>Calculated Deposition</b>	<b>Concentration of Sulfate in Snow (ng H<sub>2</sub>SO<sub>4</sub> / g H<sub>2</sub>O) due to Deposition onto Blowing Snow</b>	
Winter deposition	0.16	
Summer deposition	0.02	
Total	0.2	
Measured values in surface snow at South Pole <sup>d</sup>	~50	

<sup>a</sup> Kirchner and Delmas [1988]; Bromwich [1988]; Tzeng *et al.* [1993].

<sup>b</sup> Schwerdtfeger [1970].

<sup>c</sup> Bodhaine *et al.* [1986].

<sup>d</sup> Kirchner and Delmas [1988]; Legrand [1987].

product of the scale height of blowing snow  $H$  (m) and the density of blowing snow  $\delta$  ( $\text{g m}^{-3}$ ). A value of  $1 \text{ g m}^{-3}$  (similar to that of a boundary layer cloud) is used for  $\delta$ . The variables  $A$ ,  $H$ , and  $f$  vary significantly from summer (November through February) to winter (March through October), so a separate calculation is done for each time period (Table 3).

The blowing snow extends in height only a few meters in summer, but the smaller particles of winter can be blown much higher. We observed on occasion, during the winter blizzards at South Pole, that most of the visual obscuration of the sky due to blowing snow was above the top of a 23-m tower, but we do not know how much higher the blowing snow actually extended. For our winter calculation we therefore use a generous estimate of 200 m for scale height.

The average annual accumulation at the South Pole is about  $8 \text{ g cm}^{-2} \text{ yr}^{-1}$  [Kirchner and Delmas, 1988]. About 80% of the accumulation occurs in the winter [Bromwich, 1988; Tzeng *et al.*, 1993], so that winter and summer accumulation are about  $6.4$  and  $1.6 \text{ g cm}^{-2}$ , respectively. Our estimate for the sulfate content of snow,  $C$ , due only to aerosol deposition while the snow is blowing, is  $0.2 \text{ ng}$  of  $\text{H}_2\text{SO}_4$  per gram of snow (Table 3). The sulfate concentration in ground snow and ice is much larger, about  $50 \text{ ng g}^{-1}$  [Legrand, 1987; Kirchner and Delmas, 1988], so that deposition of aerosol particles by diffusion to blowing snow probably accounts for less than 1% of the total.

## Summary and Conclusions

The number size-distribution of ambient aerosol at South Pole peaks at  $0.13 \mu\text{m}$  and the volume size-distribution peaks at  $0.17 \mu\text{m}$ . Diffusion within porous snow appears to be the primary mechanism for deposition by filtering for particles less than  $0.6 \mu\text{m}$  dry diameter, and another mechanism (probably impaction) appears to become significant for larger particles. Deposition occurs with an  $e$ -folding time of 1 to 3 s depending on particle size, which corresponds to an estimated  $e$ -folding depth of 0.5–1 cm for typical air velocities in snow. Complete removal of aerosol particles does not occur at residence times of up to 20 s, possibly indicating a small degree of reentrainment or new particle formation. However, the number density of interstitial aerosol at 20 s is less than one thousandth that of ambient, so it should cause negligible smoothing of the sulfate record in ice cores.

Classical filter theory, Fuchs filter theory, and membrane filter theory all correctly describe filtering by snow as dominated by diffusion but quantitatively underpredict filter efficiency by about a factor of 10. This difference may be due in part to poor characterization of the snow itself in terms of grain shape and size and pore shape and size.

If Cunningham and Waddington's [1993] calculations of airflow rates and residence times are correct, our results support their model estimates for the dry deposition flux of nss sulfate of about  $3 \text{ kg SO}_4 = \text{km}^{-2} \text{ yr}^{-1}$ . Although they underpredict filter efficiency, the residence times from their air flux model are long enough to deposit virtually all the particles so that an increase in efficiency would not greatly increase their modeled deposition of sulfate. However, decreasing the model's permeability to the value we measured in surface snow would reduce the modeled flux to about  $0.7 \text{ kg SO}_4 = \text{km}^{-2} \text{ yr}^{-1}$ .

Further studies are required to determine accurately the dry deposition flux for sulfate. A more realistic representation of

particle filtering by snow could be attained by obtaining a more thorough characterization of the snow. Davis's micrographs show snow to be granular rather than fibrous and the pore space to vary greatly in morphology and dimension. Acquiring micrographs of the snow at South Pole would also be useful in characterizing the snow in the particular filters used in this study.

Perhaps more importantly, further investigation of air movement within surface snow is necessary to more reliably determine the sulfate flux. Uncertainty exists in several areas: snow permeability, the residence time of air within the snow, and the velocity of air within the snow. Residence time depends on the path length of the pore space. Tortuosity might be studied by drawing a gaseous tracer through a snow filter to determine a distribution of true path lengths and residence times. Natural air velocities and volumetric flux may be calculated from the pressure distribution measured by placing pressure transducers on the snow surface along the direction of airflow as done by Albert and Hardy [1995]. Similar filtering experiments using gas detectors rather than particle detectors would be useful to study deposition and reentrainment of reversibly deposited species.

A major consequence of the apparent importance of wind pumping and diffusion of interstitial aerosol within ground snow is that the dry deposition rate would be controlled by the rate of delivery of aerosol and the residence time of air within the pore spaces. Sulfate flux to the snow is thus a function of wind speed and surface roughness as well as atmospheric concentration. Determination of an air-snow transfer function for the paleoclimate records stored in ice is therefore complex. The atmospheric aerosol number concentration at South Pole in summer is much larger than in winter, but wind speed  $u$  is a factor of 2 higher in winter. Since deposition should be proportional to  $u^2$ , variations in winter aerosol may be disproportionately represented in the ice core record. Wind speed and sastrugi have likely changed during glacial-interglacial cycles, because of the greater meridional temperature gradient during glacial times. Ice cores drilled at locations where the wind is weak, such as at Summit in Greenland, and along the East Antarctic ridge (e.g., Dome C, Dome A) would minimize this complication.

## Appendix: Filter Theory

Several models have been developed to describe removal of particles from air by filters [Pich, 1966; Fuchs, 1964]. Deposition mechanisms considered by various authors include diffusion, inertial impaction, interception, and sedimentation. Diffusion is due to Brownian motion of particles. Impaction occurs when the inertia of a particle in an airstream carries it into an object as the airstream flows around it. Interception occurs when particles moving with the airstream are large enough to collide with an object as they flow around it. Sedimentation is due to gravitational settling of particles to a surface. Diffusion and impaction are considered to be the primary mechanisms for deposition of submicrometer particles to filters. We consider three filter theory models: Fuchs' filter theory for dense filters (small ratio of pore space radius to snow grain radius ( $h/R$ )), classical filter theory for high-porosity filters (large  $h/R$ ), and diffusion of particles to the walls of a tube. The value of  $h/R$  in our snow filters is 1.7, but the porosity is in the range 0.5 to 0.7, rather low in comparison to fibrous filters, so either Fuchs' theory or

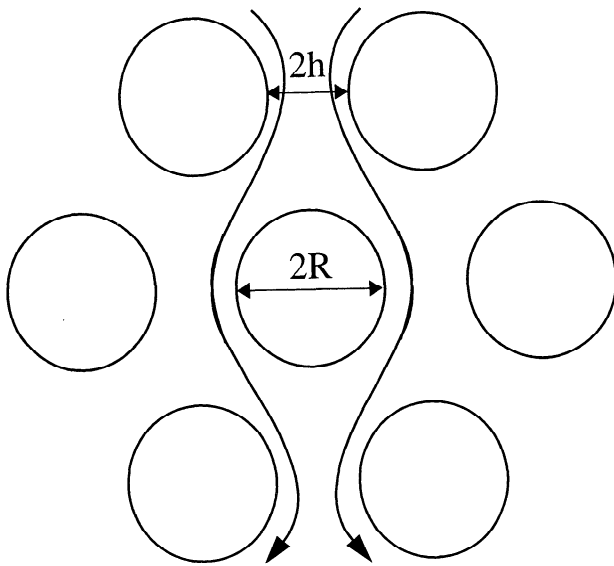


**Figure 12.** A cross-section representation of Fuchs' model filter. The cylindrical fibers are arranged in a staggered array. Fiber diameter is  $2R$  and the horizontal distance between fibers, the pore space, is  $2h$ . Laminar airflow is represented by the arrows.

classical theory may be most appropriate. All three theories overpredict particle survival time, as shown in Figure 9.

### Dense Fibrous Filters

*Fuchs* [1964] calculated fields of airflow through curved capillaries formed by the interstices of a staggered array of cylinders (Figure 12). (This modest degree of tortuosity is included in the model.) Aerosol particles are assumed to follow the flow lines of the air, so the total number of particles passing a layer per unit time is determined. The "efficiency" of a single layer is defined as the fraction of incident particles that are deposited onto that layer. The efficiencies for deposition by diffusion and interception are calculated by defining a distance from a cylinder within which all particles will be deposited (for diffusion it is the width of the diffusive boundary layer; for interception it is the radius of the particle). Flow velocity is calculated for this region, and the product of this velocity and the concentration of incident particles,  $n$  ( $\text{cm}^{-3}$ ), gives the efficiency  $E_L$  for the single layer for a single mechanism, defined as

$$E_L = \Delta n/n, \quad (14)$$

where  $\Delta n$  is the number of particles deposited in this layer by this one mechanism.

The efficiency for deposition by impaction is calculated using the Stokes number (the ratio of the stop distance of the particle to the radius of curvature of the flow line around an object) [*Fuchs*, 1964, p. 138] as for the case of impactor instruments but turning the flow lines through smaller angles than the  $90^\circ$  typically used in impactors. The efficiency for deposition by sedimentation is calculated using the settling velocity (derived by setting the Stokes drag force, i.e., the resisting force imposed on a moving particle by air, equal to the force of gravity [*Reist*, 1993, p. 59]) to determine  $\Delta n$  in equation 14.

Given the efficiency for a single layer for a given mechanism, *Fuchs* estimates the efficiency for the total filter thickness by calculating the particle concentration  $n_t$  in air after filtration (subject only to this one mechanism) as

$$n_t = n_0 \exp(-E_L Z/L), \quad (15)$$

where  $Z$  is the thickness of the whole filter,  $L$  is the thickness of a layer of the filter, and  $n_0$  is the concentration of particles in ambient air incident on the filter. The total efficiency for a multiple-layer filter (still considering one mechanism only) is then

$$E_t = 1 - (n_t/n_0) = 1 - \exp(-E_L Z/L). \quad (16)$$

Filtration can also be conveniently expressed in terms of a deposition coefficient  $\alpha$ , with units of inverse length, as

$$n_t = n_0 \exp(-\alpha Z), \quad (17)$$

where  $\alpha = E_L/L$ . *Fuchs* does not attempt to compute the efficiency for simultaneous deposition by all the mechanisms but states "All that can be said of the net efficiency by all mechanisms is that it is greater than each of the individual components but less than their arithmetical sum."

For our study, the most relevant mechanism is diffusion, for which *Fuchs*' equation (40.18) gives

$$\alpha = \frac{2D^{2/3}}{3^{1/6} U_f^{2/3} R h^{2/3} (1 + h/R)^{5/3}}, \quad (18)$$

where  $D$  is the diffusion coefficient (which depends on aerosol particle diameter) and  $U_f$  is the face velocity (the velocity of air incident on the filter entrance). The corresponding survival time  $\tau$  is

$$\tau = (U_i \alpha)^{-1}, \quad (19)$$

where  $U_i$  is the average velocity within the filter, related in *Fuchs*' model to  $U_f$  by

$$U_i = (1 + R/h)U_f. \quad (20)$$

The survival time for diffusion then becomes

$$\tau = \frac{3^{1/6} h^{5/3} (R+h)^{2/3}}{2(U_f D^2 R^2)^{1/3}}. \quad (21)$$

### Classical Filter Theory for High-Porosity Filters and Diffusion Within a Tube

Classical filter theory [*Fuchs*, 1964; *Pich*, 1966] determines the velocity field around an isolated fiber from which the particle deposition for each mechanism is calculated for that fiber. The influence of neighboring fibers and the effect of deposition occurring simultaneously by two or more mechanisms are approximated empirically. The efficiency of the whole filter is derived from the deposition per unit length of fiber per second and the total length of fiber contained in the filter.

Aerosol deposition by diffusion to the walls of a tube, the model used by CW, is reviewed by *Reist* [1993, pp. 152-155, Figure 10.4]. The remaining discussion focuses on *Fuchs*' theory.

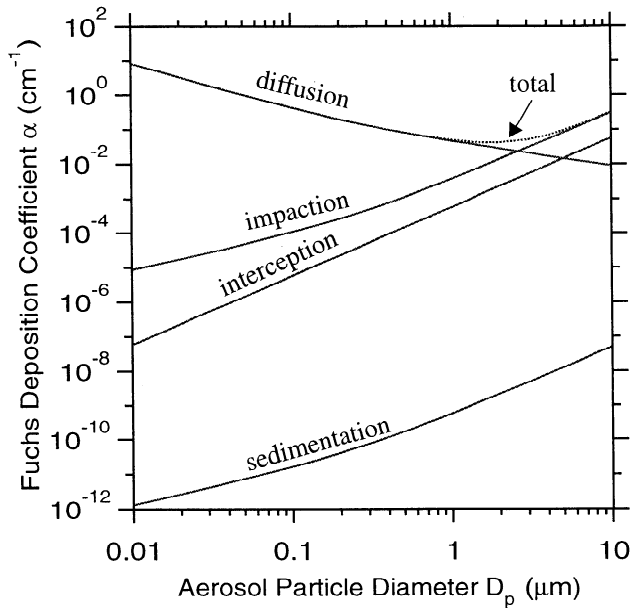


**Figure 13.** Fuchs' deposition coefficient  $\alpha$ , for four different mechanisms, as functions of aerosol particle diameter  $D_p$ . Diffusion and impaction are the main mechanisms of deposition for particles of diameter 0.1-10  $\mu\text{m}$ . The calculation is for a snow filter with face velocity  $U_f = 0.5 \text{ cm s}^{-1}$ ,  $R = 80 \mu\text{m}$ , and  $h = 130 \mu\text{m}$ .

**Representation of Snow in Filter Theory**

The filter efficiency estimated by these models is dependent on characteristics of the aerosol particles, the filter, and the filtration process. Aerosol particles are assumed to be round and rigid and deposition is dependent on the particle diameter ( $D_p$ ). Filtration efficiency also depends on the face velocity

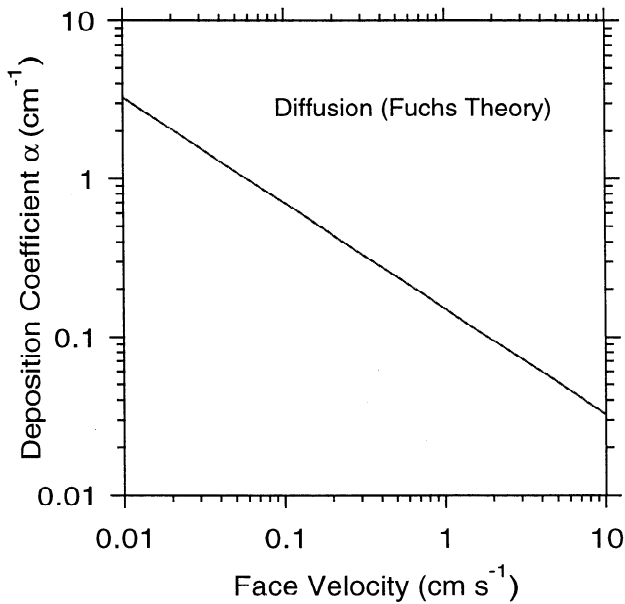


**Figure 14.** The dependence of Fuchs' deposition coefficient  $\alpha$ , for diffusion, on airflow rate (face velocity). Filter efficiency decreases with increasing flow rate because the residence time is decreased. Calculation is for a snow filter with  $R = 80 \mu\text{m}$ ,  $h = 130 \mu\text{m}$ , and  $D_p = 0.17 \mu\text{m}$ .

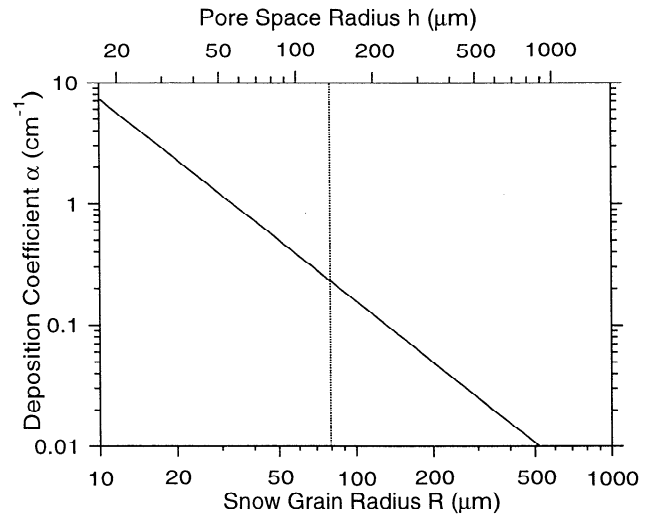


**Figure 15.** The dependence of Fuchs' deposition coefficient  $\alpha$ , for diffusion, on fiber radius (snow grain radius). Calculation is for a snow filter with  $U_f = 0.5 \text{ cm s}^{-1}$  and  $D_p = 0.17 \mu\text{m}$ . The snow density is held constant so that the pore space radius  $h$  (top scale) is proportional to  $R$ . The effective grain radius for diffusion, for south polar snow, 79  $\mu\text{m}$ , is indicated by the vertical line.

( $U_f$ ), the length of the filter ( $Z$ ), fiber radius ( $R$ ), and the size of the pore space characterized by the radius of the capillary or half the interfiber distance ( $h$ ) (Figure 12). The deposition coefficient  $\alpha$  depends on all these variables with the exception of  $Z$ . Understanding how these variables characterize filter efficiency is necessary for interpretation of data in terms of the models. Characterization studies were performed for the models using a typical snow filter:  $R = 80 \mu\text{m}$ ,  $h = 134 \mu\text{m}$ ,  $U_f = 0.5 \text{ cm s}^{-1}$ ,  $D_p = 0.17 \mu\text{m}$ . The sensitivity of the calculated efficiency to a given parameter was determined by varying that parameter over an appropriate range while maintaining the others constant.

The effect of particle size is shown for Fuchs' theory for a typical snow filter in Figure 13 where the deposition coefficient  $\alpha$  (equation 17) for each mechanism is plotted as a function of  $D_p$ . Curves for each mechanism are shown as well as a curve obtained by summing the coefficients of all four mechanisms (this curve is an upper limit for total deposition). Figure 13 shows that diffusion should be the main mechanism of deposition for particles in our size range (0.1 to 1.0  $\mu\text{m}$ ), with impaction playing a minor role and with virtually no contribution from interception and sedimentation. The minimum of the total deposition coefficient in Figure 13 occurs at  $D_p \approx 2 \mu\text{m}$ . This is larger than that found by Davidson [1989] because our flow rate was about one tenth of that used in his calculation, reducing the importance of impaction in our experiment.

The calculated dependence of Fuchs' deposition coefficient  $\alpha$  on air velocity for a typical snow filter is shown in Figure 14. This coefficient is proportional to  $U_f^{2/3}$ . For face velocities in the range of our experiments (0.24 to 1.4  $\text{cm s}^{-1}$ ),  $\alpha$  varies by a factor of 3. The calculated dependence of Fuchs' deposition coefficient on fiber radius  $R$ , which for our filters corresponds to the radius of snow grains, is shown in Figure 15. The effective radius determined for snow grains in our filters, 79  $\mu\text{m}$ , is shown with the dotted line. In this

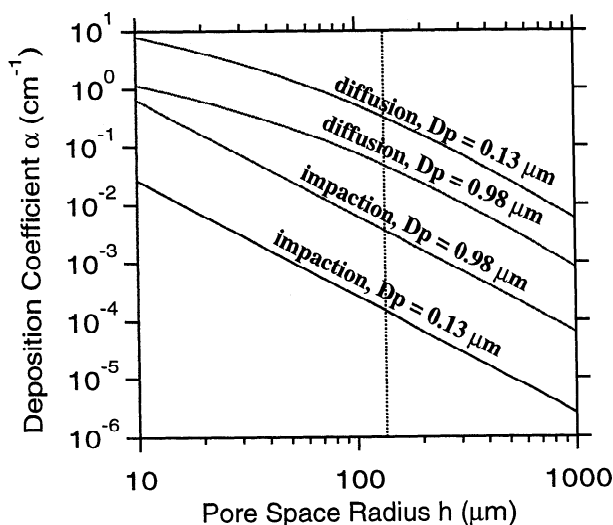


**Figure 16.** The dependence of Fuchs' deposition coefficient  $\alpha$ , for diffusion and impaction, on pore space size. Curves are shown for impaction and diffusion for the number-mode diameter of the aerosol particle size distribution,  $D_p = 0.13 \mu\text{m}$ , and for the largest size measured,  $D_p = 0.98 \mu\text{m}$ . Diffusion is seen to dominate even for the largest particles studied (near the high end of the accumulation mode). Calculation is for a snow filter with  $U_f = 0.5 \text{ cm s}^{-1}$  and  $R = 80 \mu\text{m}$ . The estimated effective pore space radius for south polar snow,  $134 \mu\text{m}$ , is indicated by the vertical line.

calculation the density is held constant while varying  $R$ , so that the pore space radius  $h$  also varies to maintain the ratio  $h/R$  constant. Filtering efficiency increases with decreasing  $R$  because of the increased surface area of filter material available for aerosol particle diffusion as well as shortened distances within the pore space required for diffusion.

The deposition coefficient as a function of pore space radius  $h$  is shown in Figure 16. Larger  $h$  corresponds to lower density. However, it is not possible to identify a unique density from values of  $h$  and  $R$  except for a monodispersion, because for a size distribution we obtain effective values  $h_e$  and  $R_e$  (equations 2 and 3), for which the weighting is not by volume. Diffusion and impaction coefficients are plotted for aerosol particle diameters at the mode and upper end of our ambient number distribution,  $0.13$  and  $0.98 \mu\text{m}$ . Decreasing  $h$  by half from  $134$  to  $67 \mu\text{m}$  leads to a threefold increase in  $\alpha$  for diffusion. Filter efficiency is thus quite sensitive to uncertainty in  $h$ , which is the least well-defined variable for our snow filters.

**Acknowledgments.** We thank Robert Davis (Cold Regions Research and Engineering Laboratory) for digitized plane sections of snow and for advice on how to estimate pore space sizes. We also thank Dave Morse for snow permeability measurements. Rich Brandt, Jim Cunningham, Brian Swanson, Ed Waddington, and Von Walden provided technical support and many useful discussions. The personnel at Amundsen-Scott South Pole Station provided logistical support. Eric Wolff and Charles Raymond reviewed the first draft. This work was supported by National Science Foundation grants OPP-91-20380 and OPP-94-21096 and by a Department of Energy Global Change Graduate Fellowship to S.L.H.

## References

Albert, M.R., and J.P. Hardy, Ventilation experiments in a seasonal snow cover, in *Biogeochemistry of Seasonally Snow-Covered Catchments*, IAHS Publ., 228, 41-49, 1995.

- Albert, M.R., E.D. Arons, and R.E. Davis, Firn properties affecting gas exchange at Summit, Greenland: Near-surface ventilation possibilities, in *Processes of Chemical Exchange Between the Atmosphere and Polar Snow*, edited by E.W. Wolff and R.C. Bales, NATO ASI Ser. I, in press, 1996.
- Anderson, T.L., G.V. Wolfe, and S.G. Warren, Biological sulfur, clouds and climate, in *Encyclopedia of Earth System Science*, edited by W. Nierenberg, pp. 363-376, Academic, San Diego, Calif., 1992.
- Bergin, M.H., J.L. Jaffrezo, C.I. Davidson, R. Caldow, and J.E. Dibb, Fluxes of chemical species to the Greenland ice sheet at Summit by fog and dry deposition, *Geochim. Cosmochim. Acta*, 58, 3207-3215, 1994.
- Bergin, M.H., C.I. Davidson, J.L. Jaffrezo, J.E. Dibb, R. Hillamo, H.D. Kuhns, and T. Makela, The contribution of wet, fog, and dry deposition to the summer  $\text{SO}_4^{2-}$  flux at Summit, Greenland, in *Ice Core Studies of Global Biogeochemical Cycles*, NATO ASI Ser. I, edited by R.J. Delmas, vol. 30, pp. 121-138, Springer-Verlag, New York, 1995.
- Bodhaine, B.A., J.J. DeLuise, J.M. Harris, P. Houmère, and S. Bauman, Aerosol measurements at the South Pole, *Tellus*, 38B, 223-235, 1986.
- Bromwich, D.H., Snowfall in high southern latitudes, *Rev. Geophys.*, 26, 149-168, 1988.
- Carman, P.C., *Flow of Gases Through Porous Media*, Academic Press, San Diego, Calif., 1956.
- Charlson, R.J., J.E. Lovelock, M.O. Andreae, and S.G. Warren, Oceanic phytoplankton, atmospheric sulfur, cloud albedo and climate, *Nature*, 326, 655-661, 1987.
- Colbeck, S.C., Air movement in snow due to windpumping, *J. Glaciol.*, 35, 209-213, 1989.
- Covert, D.S., and J. Heintzenberg, Size distributions and chemical properties of aerosol at Ny Alesund, Svalbard, *Atmos. Environ.*, 27A, 2989-2997, 1993.
- Cunningham, J., and E.D. Waddington, Air flow and dry deposition of non-sea salt sulfate in polar firn: Paleoclimatic implications, *Atmos. Environ.*, 27A, 2943-2956, 1993.
- Davidson, C.I., Mechanisms of wet and dry deposition of atmospheric contaminants to snow surfaces, in *The Environmental Record in Glaciers and Ice Sheets*, Dahlem Konferenzen, edited by H. Oeschger and C.C. Langway, pp. 29-51, John Wiley, New York, 1989.
- Fuchs, N.A., *The Mechanics of Aerosols*, Dover, New York, 1964.
- Gjessing, Y.T., The filtering effect of snow, in *Proceedings of the Symposium on Isotopes and Impurities in Snow and Ice*, IAHS Publ. 118, pp. 199-203, Int. Assoc. of Hydrol. Sci., Gentbrugge, Belgium, 1977.
- Gow, A.J., On the accumulation and seasonal stratification of snow at the South Pole, *J. Glaciology*, 5, 467-477, 1965.
- Grenfell, T.C., S.G. Warren, and P.C. Mullen, Reflection of solar radiation by the Antarctic snow surface at ultraviolet, visible, and near-infrared wavelengths, *J. Geophys. Res.*, 99, 18,669-18,684, 1994.
- Heintzenberg, J., and M. Rummukainen, Airborne particles in snow, *J. Glaciology*, 39, 239-244, 1993.
- Hogan, A.W., Meteorological transport of particulate material to the South Polar Plateau, *J. Appl. Meteorol.*, 18, 741-749, 1979.
- Hogan, A.W., and S. Barnard, Seasonal and frontal variation in Antarctic aerosol concentrations, *J. Appl. Meteorol.*, 17, 1458-1465, 1978.
- Kirchner, S., and R.J. Delmas, A 1000 year glaciochemical study at the South Pole, *Ann. Glaciol.*, 10, 80-84, 1988.
- Komhyr, W.D., An aerosol and gas sampling apparatus for remote observatory use, *J. Geophys. Res.*, 88, 3913-3918, 1983.
- LaChapelle, E.R., *Field Guide to Snow Crystals*, p. 15, Int. Glaciol. Soc., Cambridge, England, 1992.
- Legrand, M.R., Chemistry of Antarctic snow and ice, *J. Phys. Colloq. Suppl.*, 48, 77-86, 1987.
- Legrand, M.R., Sulphur-derived species in polar ice: A review, in *Ice Core Studies of Global Biogeochemical Cycles*, edited by R.J. Delmas, vol. 30, NATO ASI Ser. I, Springer-Verlag, New York, 1995.
- Legrand, M.R., and R.J. Delmas, Soluble impurities in four Antarctic ice cores over the last 30,000 years, *Ann. Glaciol.*, 10, 116-120, 1988.
- Legrand, M.R., R.J. Delmas, and R.J. Charlson, Climate forcing implications from Vostok ice-core sulphate data, *Nature*, 334, 418-420, 1988.
- Maenhaut, W., and W.H. Zoller, Concentration and size distribution of particulate trace elements in the South Polar atmosphere, *J. Geophys. Res.*, 84, 2421-2431, 1979.

- Mayewski, P.A., L.D. Meeker, S. Whitlow, M.S. Twickler, M. Morris, R.B. Alley, P. Bloomfield, and K. Taylor, The atmosphere during the Younger Dryas, *Science*, 261, 195-197, 1993.
- Mulvaney, R., and D.A. Peel, Anions and cations in ice cores from Dolleman Island and the Palmer Land Plateau, Antarctic Peninsula, *Ann. Glaciol.*, 10, 121-125, 1988.
- Paddon, J., *Image Processing Workbench: Application for Cold Regions Research*, CRREL Contr. Rep. DACA89-93-M-0107, Cold Regions Res. and Eng. Lab., Hanover, N.H., 1993.
- Pich, J., Theory of aerosol filtration by fibrous and membrane filters, in *Aerosol Science*, edited by C.N. Davies, pp. 223-285, Academic Press, San Diego, Calif., 1966.
- Pomeroy, J.W., T.D. Davies, and M. Tranter, The impact of blowing snow on snow chemistry, in *Seasonal Snowpacks: Processes of Compositional Change*, NATO ASI Ser. G, edited by T.D. Davies, M. Tranter, and H.G. Jones, pp. 70-113, Springer-Verlag, New York, 1991.
- Pruppacher, H.R., and J.D. Klett, *Microphysics of Clouds and Precipitation*, D. Reidel, Norwell, Mass, 1978.
- Reist, P.C., *Aerosol Science and Technology*, pp.131-159, McGraw-Hill, New York, 1993.
- Schwerdtfeger, W., The climate of the Antarctic, in *World Survey of Climatology*, vol. 14, edited by S. Orvig, p. 331, Elsevier, New York, 1970.
- Schwerdtfeger, W., *Weather and Climate of Antarctica*, Elsevier, New York, 1984.
- Shaw, G.E., Antarctic aerosols: A review, *Rev. Geophys.*, 26, 89-112, 1988.
- Tzeng, R., D.H. Bromwich, and T.R. Parish, Present-day Antarctic climatology of the NCAR Community Climate Model version 1, *J. Clim.*, 6, 205-226, 1993.
- Waddington, E.D., J. Cunningham, and S.L. Harder, The effects of snow ventilation on chemical concentrations in ice cores, in *Processes of Chemical Exchange Between the Atmosphere and Polar Snow*, edited by E.W. Wolff and R.C. Bales, NATO ASI Ser. I, in press, 1996.
- Whitby, K.T., The physical characteristics of sulfur aerosols, *Atmos. Environ.*, 12, 135-159, 1978.
- Young, N.W., Accumulation distribution in the IAGP area, Antarctica: 90°E - 150°E, *Ann. Glaciol.*, 3, 194-197, 1988.
- 
- R.J. Charlson, D.S. Covert, and S.G. Warren, Department of Atmospheric Sciences, Box 351640, University of Washington, Seattle, WA 98195.
- S.L. Harder, Department of Chemistry, Box 351700, University of Washington, Seattle, WA 98195. (email: harder@atmos.washington.edu)

(Received May 9, 1995; revised February 29, 1996; accepted February 29, 1996.)